Nanoscale

Accepted Manuscript

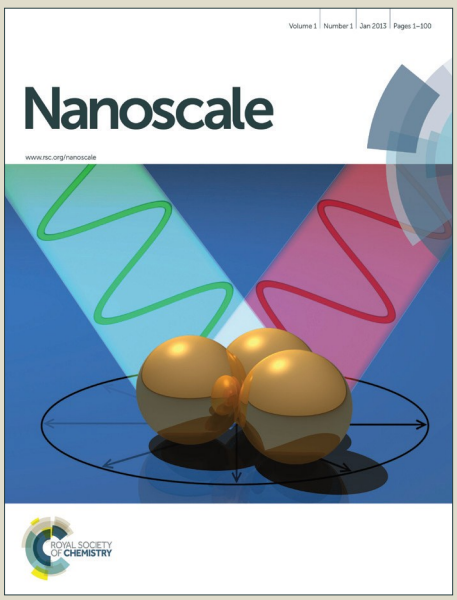

ROYAL SOCIETY OF CHEMISTRY

www.rsc.org/nanoscale

Nanoscale

RSCPublishing

PAPER

Defect-Free Thin InAs Nanowires Grown in Molecular Beam Epitaxy

Zhi Zhang,[a] Ping-Ping Chen,[b] Wei Lu,[b] and Jin Zou*[a,c]

Cite this: DOI: 10.1039/xoxxoooooox

Received ooth January 2012,
Accepted ooth January 2012

DOI: 10.1039/xoxxoooooox

www.rsc.org/

In this study, we designed a simple method to achieve the growth of defect-free thin InAs nanowires with their lateral dimension well below their Bohr radius on different substrate orientations. By depositing and annealing a thin layer of Au thin film on the (100) substrate surface, we have achieved the growth of defect-free size-uniformed thin InAs nanowires. This study provides a strategy to achieve the growth pure defect-free thin nanowires.

Introduction

III-V semiconductor nanowires have attracted extensive attentions in the recent decades due to their distinct physical properties and hence potential applications in nanoelectronics and optoelectronics.[1-3] As a key III-V semiconductor, InAs has attracted tremendous research interest due to its narrow bandgap, high electron mobility, small electron effective mass, and low-resistance ohmic contact.[4-6] The combination of these unique features and the distinct characteristics of thin nanowire have made InAs thin nanowires a promising candidate for applications in single-electron transistors, resonant tunnelling diodes, and ballistic transistors.[7-9]

Generally speaking, the most typical techniques to grow epitaxial III-V nanowires are metal-organic chemical vapor deposition,[10-12] molecular beam epitaxy (MBE)[13-16] and chemical beam epitaxy[17] through the vapor-liquid-solid mechanism[18] or vapor-solid-solid mechanisms.[19, 20] From their structural point of view, although the zinc-blende structure is energetically favorable for the III-V bulk materials, III-V nanowires can adopt the wurtzite structure as well due to its low surface energy.[21] Consequently, III-V nanowires tend to contain planar defects due to their small energetic differences of the stacking sequences in zinc-blende and wurtzite structures along their growth directions of $<111>_B/<000\bar{1}>$.[22] For nanowires to be practically useful, it is critically important to control their structural quality. Both theoretical prediction[21] and experimental results[23-25] have shown that thin nanowires prefer to form wurtzite structure. Therefore, small catalysts provide a strategy to improve the wurtzite structural quality of nanowires. Inspired by this idea, Shtrikman *et al*.[26] employed different substrate orientations in order to form small catalysts due to their different uneven substrate surfaces. However, the induced GaAs nanowires contained much larger diameters in their bottom due to possible nanowire lateral growth, and hence the thin GaAs nanowires with defect-free wurtzite structure have not been yet achieved. On the other hand, Pan *et al*.[27] proposed that a two-step catalyst thin film annealing procedure consisting of a low-temperature annealing for 10 hours and a high-temperature annealing for 20 min. Under this long-period of annealing process, small Ag catalysts with uniform sizes were achieved to induce the growth of thin nanowires. However, there are also many irregular nanostructures grown simultaneously with the nanowires. In addition, this long annealing process is time-consuming.

Although Au catalysts may affect the performance of III-V nanowires[28] and great progress has been made to explore the possibility of catalyst-free growth of III-V nanowires,[29-31] Au-assisted catalytic growth is still considered as an easy and cost-efficient approach to induce III-V nanowires. Based on our previous study,[24] we demonstrated that by depositing and annealing a comparatively thick Au catalyst film, both thin and thick InAs nanowires were induced simultaneously on the substrate due to the Ostwald ripening effect.[32] The thin nanowires have defect-free wurtzite structure, while those simultaneously grown thick nanowires tend to contain planar defects along their growth directions. In addition, our detailed investigations indicated that Au thin film thickness and annealing temperature have great effect on the catalyst size and catalyst density, that is, thin Au film thickness and low annealing temperature lead to the formation of small catalyst droplets with relatively high density.[33] In this regard, it is necessary to achieve the growth of defect-free and size-uniformed thin InAs nanowires. This is particularly essential for the lateral dimension of the thin nanowires is comparable to and/or smaller than the InAs Bohr radius (~34 nm),[34] in which the quantum confinement effects can be expected in these thin nanowires.

In this study, we demonstrate a simple approach to grow defect-free and size-uniform thin InAs nanowires by depositing and annealing a thin Au film into catalysts with small sizes. Based on our detailed structural characterization, the fundamental reason behind of our success of securing defect-free thin InAs nanowires on the (100) substrate is presented.

Experimental

The InAs nanowires were simultaneously grown on the GaAs (111) and (100) substrates in a Riber 32 MBE system using a thin Au film as catalysts. Both substrate surfaces were first degassed in the MBE preparation chamber at 250 °C, then transferred to the growth chamber to be thermally deoxidized at 580 °C. After that, a thin GaAs buffer layer was grown on each of GaAs substrates at 560 °C to achieve atomically flat surface. Both substrates were then transferred back to the preparation chamber, and a ~ 0.5 nm thick thin Au layer was deposited on the top of the GaAs buffer layer by vacuum thermal evaporation. The Au-coated GaAs substrates were finally transferred to the growth chamber, and annealed at relatively low temperature of 500 °C for 5 min under As ambient to agglomerate the Au thin film into nanoparticles. The thin Au film transforming into nanoparticles is a simple and cost-efficient approach to prepare Au catalysts.[35, 36] After the annealing, the substrate temperature was lowered to 350°C and the indium source was introduced to initiate the InAs nanowire growth with a V/III ratio of ~20.

The morphological characteristics of the as-grown InAs nanowires and substrate surfaces were investigated by scanning electron microscopy (SEM, JEOL 7800F, operated at 10 kV), and their detailed structural characteristics were investigated by transmission electron microscopy (TEM, Philips Tecnai F20, operated at 200 kV). Individual nanowires for TEM investigation were prepared by ultrasonicating the as-grown nanowire samples in ethanol and then dispersing individual nanowires onto the holey carbon films supported by Cu grids.

Results and discussion

Fig. 1 shows the SEM investigations of InAs nanowires grown on GaAs substrates with different orientations. Fig. 1a is a top-view SEM image of nanowires grown on the $(111)_B$ substrate, in which both white dots and inclined nanowires with irregular morphology can be observed. To understand the growth status of these nanostructures, side-view SEM investigation was performed. An example is shown in the Fig. 1b, in which the length of nanowires can be estimated as ~4 μm and the density of the nanowires can be established as ~7/μm^2. As can be seen, apart from some thin free-standing vertical nanowires, the majority of nanowires (> 90%) tend to stick to each other, leading to irregular morphology. Both top-view and side-view SEM analysis indicate that the nanowire density is very high. Based on our previous investigations,[33] a low-temperature annealing of a thin Au film can lead to the formation of a high density of catalyst droplets with small diameters, while a high-temperature annealing of a thick Au film then result in the formation of a low density of catalyst droplets with large diameters. In this regard, the thin nanowires with a high density grown on the GaAs $(111)_B$ substrate can be attributed to the effects of annealing a thin Au catalyst film.

Similar SEM investigations were performed on the nanowires grown on the GaAs (100) substrate. Fig. 1c is a top-view SEM image, in which nearly all the nanowires were inclined with respect to the substrate surface, and the nanowire morphology is much better than their counterparts grown on the GaAs $(111)_B$ substrate. Fig. 1d is a cleavage side-view SEM image, in which the majority of nanowires were inclined with respect to the substrate surface and vertical nanowires can be occasionally observed as well. Based on crystallography and the angle between the inclined nanowires and substrate normal, the growth direction of those inclined nanowires can be determined as two equivalent <111> directions, while those vertical nanowires have their growth direction being <100>. The lengths of these nanowires can be established as ~3.5 μm for <111> nanowires and ~2 μm for <001> nanowires. It can be noted that the density of nanowires grown on the GaAs (100) substrate is ~2/μm^2, which is much lower than that on the $(111)_B$ substrate. Since thin nanowires tend to be bent easily, when the nanowire density is high, those bending nanowires may stick to each other, and leads to the formation of irregular morphology.[37] Therefore, the low nanowire density is responsible for the better nanowire morphology.

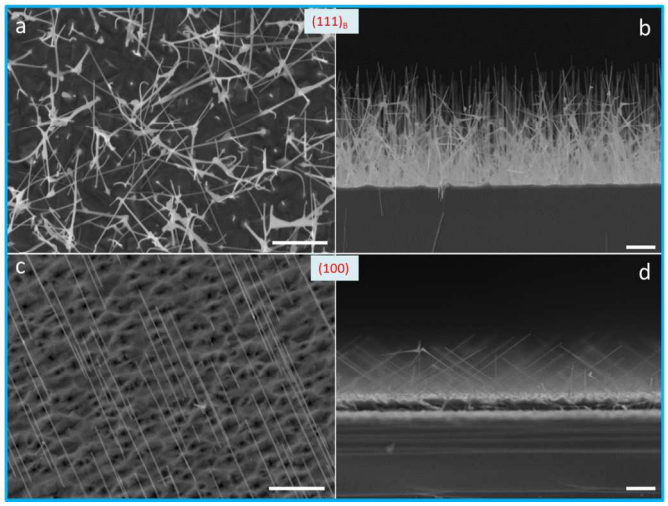

Fig. 1 (a, b) Top-view and side-view SEM images of InAs nanowires grown on the $(111)_B$ substrate, respectively. (c, d) Top-view and side-view SEM images of InAs nanowires grown on the (100) substrate, respectively. All the scale bars represent 1 μm.

To understand the morphology and structural characteristics of these thin free-standing nanowires, detailed TEM investigations were performed. Fig. 2a shows the overview of a typical vertical nanowire grown on the GaAs $(111)_B$ substrate, in which the nanowire has an uniform and small diameter (~20 nm), and no tapering caused by the nanowire lateral growth[10] was observed. To understand their crystal structure and structural quality, high-resolution TEM (HRTEM) investigations were carried out on the entire nanowire. Fig. 2b shows a typical low-magnified HRTEM image taken from the middle of the nanowire, from which no lattice

defects can be observed in a large section of the nanowire. Fig. 2c is a HRTEM image taken from a section of Fig. 2b, in which the nanowire shows perfect wurtzite structure. By examining over a dozen of vertical nanowires, the uniform thin nanowire morphology and the defect-free wurtzite structure nature can be confirmed in all cases.

Similar TEM investigations were also performed on the nanowires grown on the GaAs (100) substrate. Fig. 2d shows the overview of a typical nanowire with uniform diameter of ~20 nm, which has the same size as those vertical nanowires grown on the GaAs $(111)_B$ substrate. Detailed HRTEM investigations shown in Fig. 2e and 2f indicate that such a thin nanowire has defect-free wurtzite structure as well along the entire nanowire. To confirm the morphology and structural characteristic, we examined over a dozen of nanowires grown on the GaAs (100) substrates, and we found that all the examined nanowires have uniform thin morphology with the defect-free wurtzite structure.

Based on these experimental results, the InAs nanowires have small diameter (20 ± 2 nm) with uniform morphology, and such thin nanowires have defect-free wurtzite structure which is well consistent with theoretical prediction[21] and our previous observations.[24] These results indicate that the growth of thin InAs nanowires with defect-free structure have been successfully achieved in this study.

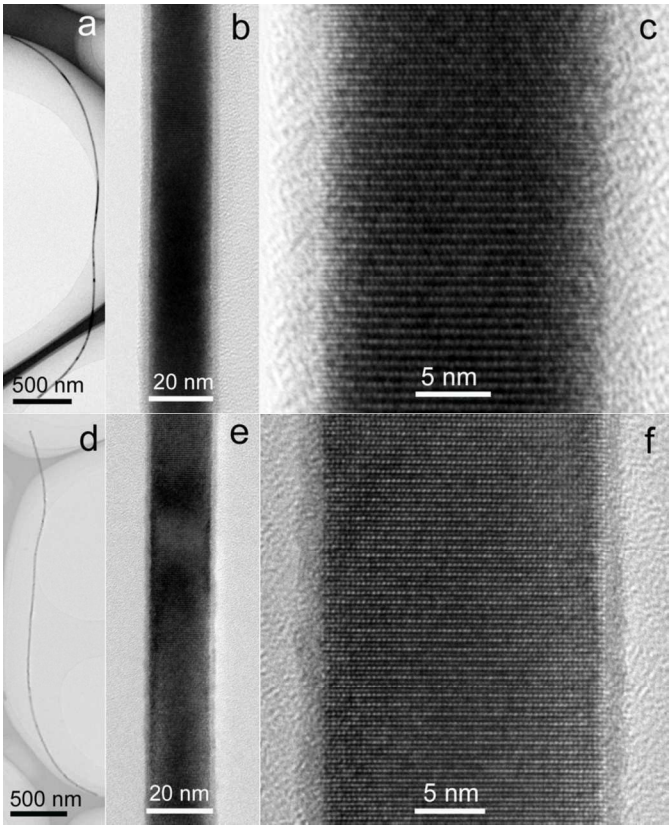

Fig. 2 TEM investigations of InAs nanowires grown on two different substrates. (a-c) Overview, low-magnified HRTEM image, HRTEM image of vertical nanowire grown on the $(111)_B$ substrate, respectively. (d-f) Overview, low-magnified HRTEM image, HRTEM image of nanowire grown on the (100) substrate, respectively.

Interestingly, the nanowire density is low for InAs nanowires grown on the GaAs (100) substrate than that on the GaAs $(111)_B$ substrate, and in turn the nanowire morphology is much better. To understand the reason of difference of nanowire densities when they are grown in different substrates, detailed surface morphology of the GaAs (100) substrate was investigated by SEM. Fig. 3a shows a magnified top-view SEM image, from which the low nanowire density characteristic can be confirmed. In addition to those inclined nanowires, many white dots (marked) can be observed as well, and these dots may be related to the projection of vertically grown nanowires or the catalysts stayed stationarily on the substrate surface. To distinguish them, the SEM specimen was tilt to 10° and the corresponding SEM image is shown in Fig. 3b. As can be noted, few of those dots in the top-view SEM image become elongated, suggesting that they are the vertically grown nanowires (marked as yellow square in Fig. 3a and yellow rectangle in Fig. 3b), which is consistent with our side-view SEM image (refer to Fig. 1d). However, most of the dots in the top-view SEM image were shown as dots in the tilted SEM image (referred to red arrows in Fig. 3b), suggesting that these catalysts indeed stayed stationarily on the substrate surface and they failed to induce nanowire growth. On this basis, the formation of lower nanowire density can be understood by the fact that many catalysts failed to induce nanowire growth. Consequently, better nanowire morphology can be achieved when they are grown on the (100) substrate due to the lower nanowire density.

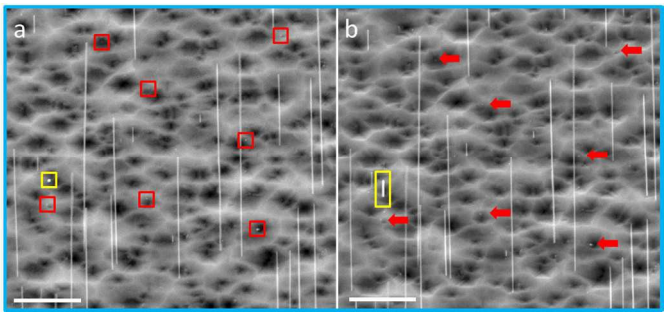

Fig. 3 SEM investigations on the nanowires grown on the (100) substrate from the same area. (a) top-view SEM image. (b) 10° tilted SEM image. All the scale bars represent 1 μm.

As mentioned earlier, vertical <100> nanowires grown on the (100) substrate were occasionally observed, so that their structural quality should be examined. Fig. 4a is a bright-field TEM image of a typical <100> nanowire, and shows that vertical <100> nanowire has similar catalyst size (~20 nm) as those wurtzite structured <0001> nanowires. To understand their crystal structure and structural quality, HRTEM investigations were performed along the entire nanowire. Fig. 4b shows a typical low-magnified HRTEM image showing no lattice defects in a large section of nanowire, and Fig. 4c is a HRTEM image taken from a section of Fig. 4b, in which the nanowire is confirmed to grow along the <100> growth direction and have defect-free zinc-blende structure. The defect-free structural quality can be explained by the fact that nanowires grown on non <111>/<0001> directions with non {111}/{0001} nanowire/catalyst

interfaces tend to be defect-free due to their required high energy barriers for the creation of stacking faults in <100> nanowires.[38, 39]

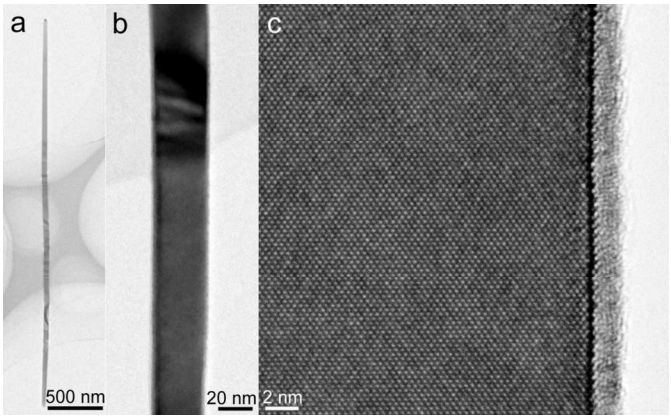

Fig. 4 TEM investigation of <100> nanowires grown on the (100) substrate. (a-c) Overview, low-magnified HRTEM image, HRTEM image, respectively.

To understand the formation of such vertical <100> nanowires, and the failure of some catalysts to induce nanowire growth, when InAs nanowires are grown on the GaAs (100) substrate, we note the following two facts. It has been well demonstrated[40, 41] that, (1) if the nanowire growth was conducted without the catalyst annealing process, vertical <100> nanowires can be induced from the intact Au/(100) interface on the (100) substrate when the critical supersaturation is reached. (2) If the growth was conducted with high temperature annealing process, the Au catalyst will etch into the substrate surface, and develop the low-energy {111} interface between the Au catalyst and (100) substrate surface, leading to the formation of <111>/<0001> nanowires on the (100) substrate. Under our growth condition, compared to the high annealing temperature (600 °C) on the (100) substrate which leads to the growth of very high nanowire density,[42] the annealing temperature (500 °C) in our work is relatively low. In this regard, the formation of Au/semiconductor {111} interface may have not been well developed for all catalysts. In addition, due to the relatively low growth temperature, it is expected that the chance of In atoms diffusing into the Au catalysts is low due to small diffusion length of group-III atoms on the (100) surface plane compared to that on the $(111)_B$ surface plane,[43] and hence it is anticipated that less catalysts have reached the supersaturation level required for the nanowire growth.[44] In this regard, only those catalysts have reached the supersaturation level and have formed well-developed interface with semiconductor surface can induce the nanowire growth since the formation of catalyst/nanowire interface is critical to the nanowire growth.[44, 45] Therefore, as a result of the low nanowire density, the morphology of thin nanowires grown on the (100) substrate can be greatly improved compared to that grown on the $(111)_B$ substrate.

Based on these experimental results and discussion outlined above, we anticipate that by depositing a thin layer of Au thin film on the substrate surface and adopting a relatively low annealing temperature, the growth of thin defect-free InAs nanowires have been successfully achieved on both GaAs $(111)_B$ substrate and (100) substrate. To test this growth strategy, we repeated the nanowire growth on other substrate orientations such as $(211)_A$ substrate and (110) substrate. It can be noted that the nanowire morphology is not comparable with that on the (100) substrate, which is due to the high density of thin nanowires grown on the $(211)_A$ and (110) substrate. Our extensive SEM (refer to Fig. 5) and TEM investigations confirmed that all those nanowires with regular morphology are thin (~20 nm) and adopt defect-free wurtzite structure (results not shown here). Specifically, when the growth was conducted on the (100) substrate surface, we can achieve the growth of defect-free wurtzite structured thin InAs nanowires with well-controlled nanowire morphology. These results suggest that the substrate orientation provide a strategy to control the morphology of nanowires.

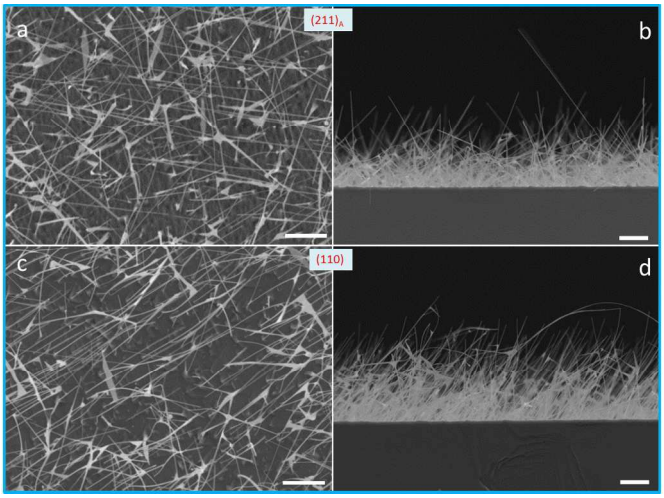

Fig. 5 (a, b) Top-view and side-view SEM images of InAs nanowires grown on the $(211)_A$ substrate, respectively. (c, d) Top-view and side-view SEM images of InAs nanowires grown on the (110) substrate, respectively. All the scale bars represent 1 μm.

Conclusions

In conclusion, we present a simple method to achieve the growth of defect-free and size-uniformed thin InAs nanowires with their lateral dimension well below their Bohr radius. By depositing and annealing a thin layer of Au thin film on the (100) substrate surface, the synthesized thin InAs nanowires have defect-free nanowire structure.

Acknowledgements

This study was financially supported by the Australian Research Council, the National Basic Research Program of China (Grant No. 2011CB925604), and the National Science Foundation of China (Grant No. 61376015, 91321311), and Shanghai Science and Technology Foundation (Grant No. 13JC1405901). Australian Microscopy & Microanalysis Research Facility is also gratefully acknowledged for providing microscopy facilities for this study.

Notes and references

[a] Materials Engineering, The University of Queensland, St. Lucia, QLD 4072, Australia

[b] National Laboratory for Infrared Physics, Shanghai Institute of Technical Physics, Chinese Academy of Sciences, 500 Yu-Tian Road, Shanghai 200083, China

[c] Centre for Microscopy and Microanalysis, The University of Queensland, St. Lucia, QLD 4072, Australia

1 X. F. Duan, Y. Huang, Y. Cui, J. F. Wang and C. M. Lieber, *Nature*, 2001, **409**, 66.

2 H. Xia, Z. Y. Lu, T. X. Li, P. Parkinson, Z. M. Liao, F. H. Liu, W. Lu, W. D. Hu, P. P. Chen, H. Y. Xu, J. Zou and C. Jagadish, *ACS Nano*, 2012, **6**, 6005.

3 N. Guo, W. D. Hu, L. Liao, S. Yip, J. C. Ho, J. D. Miao, Z. Zhang, J. Zou, T. Jiang, S. J. Wu, X. S. Chen and W. Lu, *Adv. Mater.*, 2014, **26**, 8232.

4 S. A. Dayeh, D. P. R. Aplin, X. Zhou, P. K. L. Yu, E. T. Yu and D. Wang, *Small*, 2007, **3**, 326.

5 S. L. Wright, R. F. Marks, S. Tiwari, T. N. Jackson and H. Baratte, *Appl. Phys. Lett.*, 1986, **49**, 1545.

6 A. G. Milnes and A. Y. Polyakov, *Mat. Sci. Eng. B*, 1993, **18**, 237.

7 C. Thelander, T. Martensson, M. T. Bjork, B. J. Ohlsson, M. W. Larsson, L. R. Wallenberg and L. Samuelson, *Appl. Phys. Lett.*, 2003, **83**, 2052.

8 M. T. Bjork, B. J. Ohlsson, C. Thelander, A. I. Persson, K. Deppert, L. R. Wallenberg and L. Samuelson, *Appl. Phys. Lett.*, 2002, **81**, 4458.

9 X. Zhou, S. A. Dayeh, D. Aplin, D. Wang and E. T. Yu, *Appl. Phys. Lett.*, 2006, **89**, 053113.

10 J. Zou, M. Paladugu, H. Wang, G. J. Auchterlonie, Y. N. Guo, Y. Kim, Q. Gao, H. J. Joyce, H. H. Tan and C. Jagadish, *Small*, 2007, **3**, 389.

11 H. Y. Xu, Y. Wang, Y. N. Guo, Z. M. Liao, Q. Gao, N. Jiang, H. H. Tan, C. Jagadish and J. Zou, *Cryst. Growth Des.*, 2012, **12**, 2018.

12 Y. N. Guo, H. Y. Xu, G. Auchterlonie, T. Burgess, H. J. Joyce, Q. Gao, H. H. Tan, C. Jagadish, H. B. Shu, X. S. Chen, W. Lu, Y. Kim and J. Zou, *Nano Lett.*, 2013, **13**, 643.

13 V. G. Dubrovskii, *Appl. Phys. Lett.*, 2014, **104**, 053110.

14 Z. Zhang, Z. Y. Lu, P. P. Chen, W. Lu and J. Zou, *Nanoscale*, 2015, **7**, 12592.

15 J.-H. Kang, Y. Cohen, Y. Ronen, M. Heiblum, R. Buczko, P. Kacman, R. Popovitz-Biro and H. Shtrikman, *Nano Lett.*, 2013, **13**, 5190.

16 S.-X. Shi, Z.-Y. Lu, Z. Zhang, C. Zhou, P.-P. Chen and J. Zou, *Chin. Phys. Lett.*, 2014, **31**, 098101.

17 L. E. Jensen, M. T. Bjork, S. Jeppesen, A. I. Persson, B. J. Ohlsson and L. Samuelson, *Nano Lett.*, 2004, **4**, 1961.

18 R. S. Wagner and W. C. Ellis, *Appl. Phys. Lett.*, 1964, **4**, 89.

19 A. I. Persson, M. W. Larsson, S. Stenstrom, B. J. Ohlsson, L. Samuelson and L. R. Wallenberg, *Nat. Mater.*, 2004, **3**, 677.

20 K. A. Dick, K. Deppert, T. Martensson, B. Mandl, L. Samuelson and W. Seifert, *Nano Lett.*, 2005, **5**, 761.

21 T. Akiyama, K. Sano, K. Nakamura and T. Ito, *Jpn. J. Appl. Phys.*, 2006, **45**, L275.

22 H. Y. Xu, Y. Wang, Y. N. Guo, Z. M. Liao, Q. Gao, H. H. Tan, C. Jagadish and J. Zou, *Nano Lett.*, 2012, **12**, 5744.

23 J. Johansson, K. A. Dick, P. Caroff, M. E. Messing, J. Bolinsson, K. Deppert and L. Samuelson, *J. Phys. Chem. C*, 2010, **114**, 3837.

24 Z. Zhang, Z. Y. Lu, P. P. Chen, H. Y. Xu, Y. N. Guo, Z. M. Liao, S. X. Shi, W. Lu and J. Zou, *Appl. Phys. Lett.*, 2013, **103**, 073109.

25 K. Jung, P. K. Mohseni and X. Li, *Nanoscale*, 2014, **6**, 15293.

26 H. Shtrikman, R. Popovitz-Biro, A. Kretinin, L. Houben, M. Heiblum, M. Bukala, M. Galicka, R. Buczko and P. Kacman, *Nano Lett.*, 2009, **9**, 1506.

27 D. Pan, M. Fu, X. Yu, X. Wang, L. Zhu, S. Nie, S. Wang, Q. Chen, P. Xiong, S. von Molnar and J. Zhao, *Nano Lett.*, 2014, **14**, 1214.

28 K. A. Dick and P. Caroff, *Nanoscale*, 2014, **6**, 3006.

29 Q. D. Zhuang, E. A. Anyebe, R. Chen, H. Liu, A. M. Sanchez, M. K. Rajpalke, T. D. Veal, Z. M. Wang, Y. Z. Huang and H. D. Sun, *Nano Lett.*, 2015, **15**, 1109.

30 M. J. L. Sourribes, I. Isakov, M. Panfilova, H. Liu and P. A. Warburton, *Nano Lett.*, 2014, **14**, 1643.

31 E. A. Anyebe, A. M. Sanchez, S. Hindmarsh, X. Chen, J. Shao, M. K. Rajpalke, T. D. Veal, B. J. Robinson, O. Kolosov, F. Anderson, R. Sundaram, Z. M. Wang, V. Falko and Q. Zhuang, *Nano Lett.*, 2015.

32 P. W. Voorhees, *J. Stat. Phys.*, 1985, **38**, 231.

33 H. Y. Xu, Y. N. Guo, W. Sun, Z. M. Liao, T. Burgess, H. F. Lu, Q. Gao, H. H. Tan, C. Jagadish and J. Zou, *Nanoscale Res. Lett.*, 2012, **7**, 589.

34 K. Takei, H. Fang, S. B. Kumar, R. Kapadia, Q. Gao, M. Madsen, H. S. Kim, C.-H. Liu, Y.-L. Chueh, E. Plis, S. Krishna, H. A. Bechtel, J. Guo and A. Javey, *Nano Lett.*, 2011, **11**, 5008.

35 Z. M. Liao, Z. G. Chen, Z. Y. Lu, H. Y. Xu, Y. N. Guo, W. Sun, Z. Zhang, L. Yang, P. P. Chen, W. Lu and J. Zou, *Appl. Phys. Lett.*, 2013, **102**, 063106.

36 Z. Zhang, Z. Y. Lu, P. P. Chen, W. Lu and J. Zou, *Acta Mater.*, 2015, **92**, 25.

37 X. Dai, S. A. Dayeh, V. Veeramuthu, A. Larrue, J. Wang, H. Su and C. Soci, *Nano Lett.*, 2011, **11**, 4947.

38 J. Wang, S. R. Plissard, M. A. Verheijen, L.-F. Feiner, A. Cavalli and E. P. A. M. Bakkers, *Nano Lett.*, 2013, **13**, 3802.

39 Z. Zhang, K. Zheng, Z. Y. Lu, P. P. Chen, W. Lu and J. Zou, *Nano Lett.*, 2015, **15**, 876.

40 U. Krishnamachari, M. Borgstrom, B. J. Ohlsson, N. Panev, L. Samuelson, W. Seifert, M. W. Larsson and L. R. Wallenberg, *Appl. Phys. Lett.*, 2004, **85**, 2077.

41 W. Seifert, M. Borgstrom, K. Deppert, K. A. Dick, J. Johansson, M. W. Larsson, T. Martensson, N. Skold, C. P. T. Svensson, B. A. Wacaser, L. R. Wallenberg and L. Samuelson, *J. Cryst. Growth*, 2004, **272**, 211.

42 W. Sun, Y. N. Guo, H. Y. Xu, Q. Gao, H. H. Tan, C. Jagadish and J. Zou, *Appl. Phys. Lett.*, 2013, **103**, 223104.

43 T. Takebe, M. Fujii, T. Yamamoto, K. Fujita and T. Watanabe, *J. Appl. Phys.*, 1997, **81**, 7273.

44 Z. Zhang, Z. Y. Lu, H. Y. Xu, P. P. Chen, W. Lu and J. Zou, *Nano Res.*, 2014, **7**, 1640.

45 H. J. Joyce, Q. Gao, H. H. Tan, C. Jagadish, Y. Kim, X. Zhang, Y. N. Guo and J. Zou, *Nano Lett.*, 2007, **7**, 921.

Table of Content

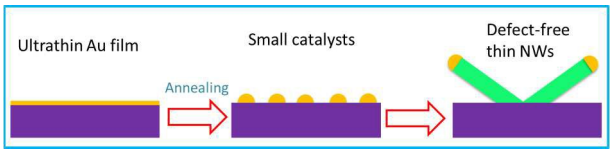

Controlled growth of defect-free thin InAs nanowires in MBE.